Journal of Alloys and Compounds 523 (2012) 134–138

Contents lists available at SciVerse ScienceDirect

Journal of Alloys and Compounds

journal homepage: www.elsevier.com/locate/jallcom

Novel asymmetric anode-supported hollow fiber solid oxide fuel cell

Dixiong Zhou, Shujun Peng, Yanying Wei, Zhong Li, Haihui Wang*

School of Chemistry & Chemical Engineering, South China University of Technology, No. 381 Wushan Road, Guangzhou 510640, China

ARTICLE INFO

Article history:
Received 12 October 2011
Received in revised form 13 January 2012
Accepted 18 January 2012
Available online 28 January 2012

Keywords:
Hollow fiber
SOFC
YSZ
Anode-supported

ABSTRACT

Ni–$(Y_2O_3)_{0.08}(ZrO_2)_{0.92}$(YSZ) anode-supported hollow fiber solid oxide fuel cell (HF-SOFC) with an outer diameter of 1.1 mm was successfully fabricated by a wet spinning/sintering process. The anode-supported hollow fiber shows a highly asymmetric structure with finger-like voids at the inner side and sponge-like pores at the outer side. Dense YSZ electrolyte layer about 6.5 μm was deposited onto the anode hollow fiber by dip coating. $La_{0.8}Sr_{0.2}MnO_{3-\delta}$ (LSM)–YSZ was acted as the composite cathode. The performance of the as-prepared HF-SOFC was tested at 650–800 °C with humidified H_2 as fuel and ambient air as oxidant, respectively. The cell provides maximum power densities of 285, 446, 549 and 708 mW cm^{-2} at 650, 700, 750 and 800 °C, respectively. At 800 °C, the fuel utilization of the maximum power output with different fuel flow rate has been calculated. The excellent performance of the cell indicates that the HF-SOFC has great potential applications in auxiliary power units (APUs) and power sources of portable devices.

1. Introduction

Solid oxide fuel cell (SOFC) is a new energy conversion device which can transform chemical energy into electrical one directly. In recent years, lots of researches have been focused on SOFC due to its fuel flexibility, environmental-friendly operation and high energy conversion efficiency [1]. There are two main kinds of geometries for SOFCs, which are planar one and tubular one [2–5]. Compared with planar design, tubular SOFC has two obvious advantages, which are high thermal stability and easy sealing. However, anode-supported tubular SOFC has long current path and relatively thick wall which results in higher anode polarization resistance and greater loss in electrical energy output [6]. Tubular SOFC with small diameter is less susceptible to crack induced by rapid heating at start-up [7,8]. Up to date, the most common technique used in fabricating micro tube for anode supporter is extrusion process [9,10] and slip casting [4,5], which are complex, unstable and time cost. Furthermore, the as-prepared anode tubes using these techniques usually have large wall thickness; the microstructure of anode cannot be controlled. Recently, a spinning/phase inversion process has been developed to fabricate ceramic micro tube membranes with thin wall thickness and asymmetric structure that greatly reduces mass transfer of the fuel and the products [11–15]. Spinning/phase inversion process can control the microstructure and porosity achievable by the optimization of the fabrication parameters [15]. At the same time, increasing activities can be found in the preparation of SOFCs in hollow fiber geometry because the hollow fiber SOFC (HF-SOFC) has high volumetric power density, good mechanical properties, good thermo-cycling behavior, and quick start-up and shut-down operations [16]. Examples are shown on the pioneering papers from the groups of Li and co-workers [17–19], Liu and co-workers [20] and Zhang et al. [21].

So far, the power density of HF-SOFC is still not so high. An anode-supported hollow fiber SOFC with YSZ electrolyte and LSM–YSZ composite cathode exhibits maximum power density of 377 mW cm^{-2} at 800 °C [20]. The main reason is that the as-prepared anode of HF-SOFC usually has low porosity, which may create high resistance to the diffusion of gaseous fuel during the operation. Therefore, to increase the electrode porosity is an effective approach to achieve high power density. Recently, a spinning/phase inversion process has been applied to fabricate ceramic hollow fiber membranes with thin wall and asymmetric structure in our group [22]. During the spinning process, a highly asymmetric structure comprised of a finger-like internal and sponge-like external layer can be prepared by using different internal and external coagulants [23].

In this study, a novel asymmetric anode-supported HF-SOFC with a diameter of 1.1 mm was fabricated by the spinning/phase inversion technology, a dense YSZ electrolyte layer ca. 6.5 μm was deposited onto the anode hollow fiber by dip coating. LSM–YSZ as composite cathode and pure LSM as cathode current collection layer were prepared by brush painting. The electrochemical characterization of the as-prepared HF-SOFC was investigated in the temperature range of 650–800 °C.

2. Experimental

The NiO–YSZ (1:1 wt%, Yitong New Material Co. Ltd., Weifang, China) asymmetric anode hollow fibers were fabricated by a wet spinning/sintering method.

* Corresponding author. Tel.: +86 20 87110131; fax: +86 20 87110131.
E-mail address: hhwang@scut.edu.cn (H. Wang).

0925-8388/$ – see front matter © 2012 Elsevier B.V. All rights reserved.
doi:10.1016/j.jallcom.2012.01.120

Table 1
Preparation conditions for NiO–YSZ hollow fiber anode supporter.

Parameter	Value
Compositions of the starting solution	
NiO–YSZ powder	60 wt%
PESf, A-300	8 wt%
NMP	30 wt%
PVP, K30	2 wt%
Spinning temperature	25 °C
Injection rate of internal coagulant	2 ml min^{-1}
Spinning pressure	0.1 bar
Air gap	0.3 cm
Sintering temperature	1250 °C
Sintering time	2 h

Polyethersulfone (PESf, A-300, BASF), N-methyl-2-pyrrolidone (NMP) (AR Grade, Kermel Chem. Inc., Tianjin, China) and Polyvinylpyrrolidone (PVP, K30, Boao Biotech Co., Shanghai, China) were served as polymer binder, solvent and dispersant, respectively. NMP and deionized water were used as the internal and external coagulant, respectively. After drying in the air at room temperature for more than 24 h, the NiO–YSZ hollow fiber precursors were sintered at 1250 °C for 2 h under static air atmosphere to remove the organic compounds. The operation conditions employed in the preparation of the NiO–YSZ hollow fiber anode supporter are summarized in Table 1.

An YSZ (TZ-8YS, 40 nm, Tosoh Co., Japan) electrolyte layer was deposited onto the anode hollow fiber by dip coating. The YSZ powder was dispersed in an organic mixture including ethanol, ethylcellulose and terpineol served as solvent, binder and plasticizer, respectively [24]. The addition of binder can prevent the electrolyte layer from cracking during drying and sintering process. A well dispersed and stable YSZ suspension was formed by stirring for several minutes, and treating by ultrasonic for 60 min. The pre-calcined anode hollow fiber was cleaned by ultrasound firstly and then was dip-coated in the YSZ suspension for 10 s and dried in the environmental atmosphere for several minutes. The dip-coating process was repeated for five times in order to ensure a full coverage of the YSZ layer with proper thickness on the anode. The NiO–YSZ/YSZ was co-sintered at 1400 °C for 4 h to make a dense electrolyte film. Finally, the LSM–YSZ (1:1 wt%) composite cathode layer and pure LSM cathode current collection layer were coated on YSZ electrolyte film via brush painting in turn, followed by heat treatment at 1000 °C for 2 h.

The microstructure of the samples was observed by a scanning electron microscopy (SEM, JEOL JSM-6490LA). The porosity of the anode was determined by Archimedes' method. The electrical conductivity of the anode was measured using the two-probe DC technique at room temperature. The electrochemical performance of the single HF-SOFC was investigated from 650 °C to 800 °C using an Arbin Electrical Load Test System (BT 2000, USA). Silver wire was served as current collector for both anode and cathode sides by a double terminal model, which was fixed by Ag paste. Humidified hydrogen (~3% H_2O, 25 °C) was used as fuel at a flow rate of 3–30 ml min^{-1} and cathode was exposed in the ambient air. Before the electrochemical test, the NiO–YSZ hollow fiber of the HF-SOFC was reduced at 600 °C for 2 h.

The porosity of the anode hollow fiber which was co-sintered at 1400 °C for 4 h before and after H_2 reduction was calculated to be approximately 35% and 46%, respectively, using the following equation (1).

$$\varepsilon = \frac{\Delta m}{V\rho_{H_2O}} \times 100\% = \frac{m_{wet} - m_{dry}}{\left(\pi/4\right)(D^2 - d^2)L\rho_{H_2O}} \times 100\% \quad (1)$$

where m_{dry} is the dry weight of anode which was treated at 120 °C for 24 h, m_{wet} is the wet weight of anode soaked in boiled water more than 48 h, and L, D, and d are the length (20 mm), outer and inner diameters of the anode fiber, respectively. The large porosity in this study can improve the mass transport within the hollow fiber anode.

The electrical conductivity measurement in this study was carried out using the two-probe DC technique at room temperature. Linear fits to the generated V–I data were used to determine fiber resistance from which the electrical conductivity of the anode (Ni–YSZ) (σ, S cm^{-1}) was estimated using the following equation (2):

$$\sigma = \frac{L}{RA_c} \quad (2)$$

where σ is the conductivity in S cm^{-1}, R is the electrical resistance, L is the fiber length, and A_c is the cross-sectional area of the hollow fiber, given by Eq. (3):

$$A_c = \frac{\pi(D^2 - d^2)}{4} \quad (3)$$

where D and d are the outer and inner diameters of the hollow fiber, respectively. Prior to measurement, the anode hollow fiber was reduced at 600 °C using flowing hydrogen for 2 h. As a result, the electrical conductivity of the anode (Ni–YSZ) fabricated in this study is measured to be 1.26×10^2 S cm^{-1}.

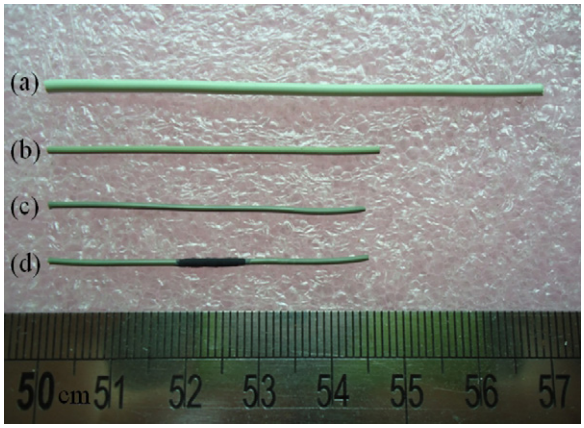

Fig. 1. Photos of anode-supported hollow fiber SOFCs: (a) anode precursor, (b) anode supporter, (c) thin electrolyte-coated anode substrate, (d) whole hollow fiber cell.

3. Results and discussion

Fig. 1 presents photos of anode-supported hollow fiber SOFCs at different stages of fabrication. Fig. 1(a) is the NiO–YSZ hollow fiber anode precursor prepared by spinning/phase inversion technique with an outer diameter of 1.5 mm. After the precursor sintered at 1250 °C for 2 h at static air atmosphere, anode supporter with good mechanical strength is shown in Fig. 1(b), the supporter with an outer diameter of 1.2 mm, shrank by 20%. Fig. 1(c) shows thin YSZ electrolyte-coated anode substrate after co-sintered at 1400 °C for 4 h with an outer diameter of 1.0 mm, it was shrunk further. Fig. 1(d) shows an image of the whole hollow fiber cell including LSM–YSZ composite cathode and pure LSM cathode current collection layer. The prepared hollow fiber SOFC was 45 mm long, with outer and inner diameters of approximately 1.1 mm and 0.8 mm, respectively, and a cathode layer of 10 mm length with an effective cathode area of 0.40 cm^2.

Fig. 2 shows the cross-sectional SEM micrographs of the HF-SOFC. As seen in Fig. 2(a) and (b), the thickness of the hollow fiber anode is ca. 175 μm and it has an asymmetric structure with a finger-like porous structure at the inner side and a sponge-like microporous structure at the outer side. The formation of such an asymmetric structure may be attributed to the fast precipitation of spinning solution in the outer deionized water coagulant and the delayed precipitation of spinning solution in the inner NMP coagulant during the spinning process [25]. The finger-like porous structure is formed at the inner side of the hollow fiber which provides the delivery channels of fuel gas transported to the electrolyte rapidly [26]. The sponge-like microporous structure near the YSZ electrolyte can provide large reduction catalysis area of H_2 and enlarge the area of the anode triple phase boundary (TPB) including the anode, electrolyte and H_2 gas, which is benefit for improving the total cell performance. The thicknesses of the finger-like porous structure and the sponge-like microporous structure are ca. 160 μm and 15 μm, respectively. The anode hollow fiber precursors sintered at 1250 °C for 2 h in order to get the ideal structure which possesses enough mechanical strength and large porosity. As we can see from Fig. 2(c), the HF-SOFC about 280 μm in thickness shows an obvious microstructure including anode, electrolyte, composite cathode and cathode current collection layer. Fig. 2(d) shows that the YSZ membrane with thickness of ca. 6.5 μm is quite dense and crack-free, which is tightly connected to both anode and cathode. As a result, it can reduce the contact resistance between the electrodes and the electrolyte.

Fig. 3 shows that X-ray diffraction (XRD) patterns of the anode inner layer (before and after reduction) are compared with the

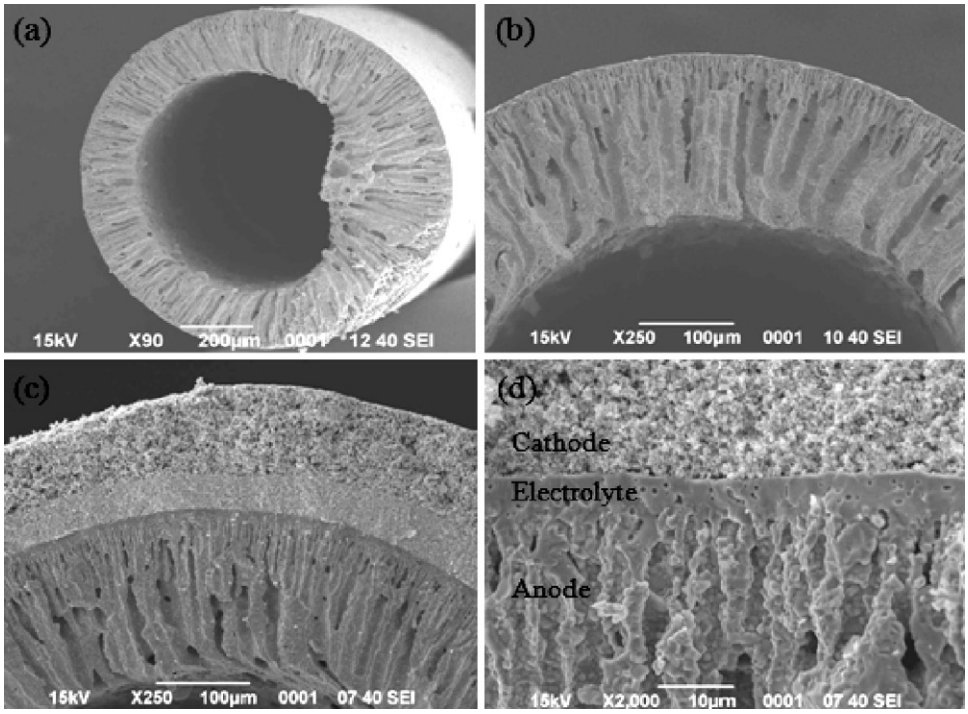

Fig. 2. SEM micrographs of the anode-supported NiO–YSZ/YSZ/YSZ–LSM/LSM HF-SOFC: (a) over view of anode, (b) cross-section of anode, (c) cross-section of cell, (d) high magnification.

original NiO and YSZ powders. Fig. 3(a) presents the XRD of original NiO–YSZ powders, which is in good agreement with the literature results [27,28]. As shown in the Fig. 3(b), no extra reflections belonging to phases other than the tetragonal phase (t-YSZ) of YSZ and the cubic phase of NiO in the NiO–YSZ hollow fiber sample. It indicates that the hollow fiber supporter is comprised of a mixture of NiO and YSZ with no appreciable formation of new phases during the spinning and sintering process. Therefore, spinning/phase inversion is an effective method in fabrication of HF-SOFCs which will not introduce any impurity. In addition, the peak intensity of the NiO–YSZ hollow fiber is stronger than the original powder, indicating that the grain size of hollow fiber is larger than the original powder due to the aggregation of the NiO–YSZ powder during sintering. The XRD of anode after reduction, as shown in Fig. 3(c), it indicates that all the NiO particles have been successfully reduced to Ni at 600 °C for 2 h using hydrogen. The XRD results indicated that the NiO was reduced to Ni thoroughly by hydrogen under the given reduction condition.

Fig. 4 shows the current–voltage characteristics of the HF-SOFC and the corresponding power densities as a function of current densities at different temperatures. As shown in Fig. 4, the open-circuit voltage (OCV) varies from 1.07 to 1.02 V from the temperature of 650–800 °C. The maximum power densities of 285, 446, 549 and 708 mW cm^{-2} are obtained at 650, 700, 750 and 800 °C, respectively. Such a result is quite encouraging and higher than previously reported values by Liu and co-workers [20], which is mainly because of the controlled microstructure of the anode, a highly asymmetric one with a finger-like porous structure and a sponge-like microporous structure. The finger-like porous structure formed

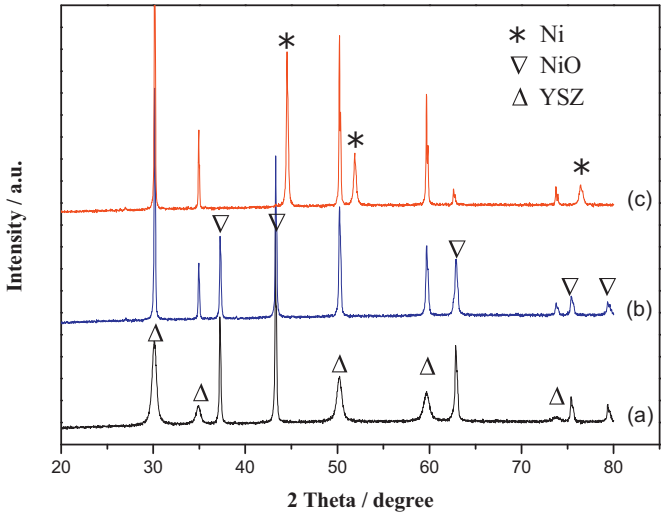

Fig. 3. XRD patterns of the (a) original NiO–YSZ powder, (b) the NiO–YSZ hollow fiber supporter and (c) Ni–YSZ hollow fiber after reduction.

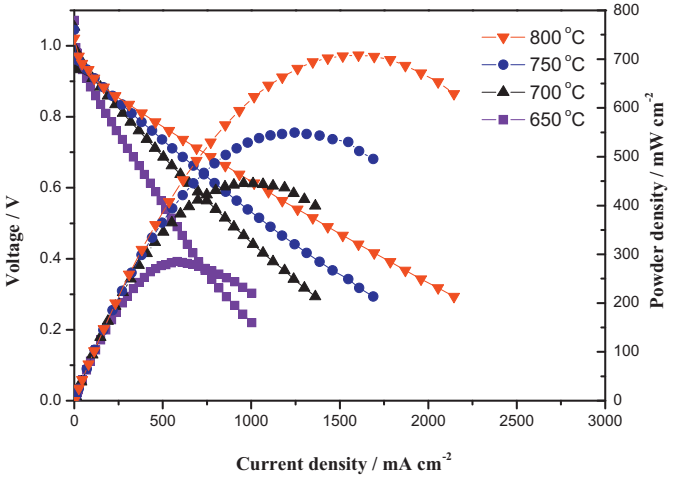

Fig. 4. Current–voltage characteristics and the corresponding power densities as a function of current densities for HF-SOFC.

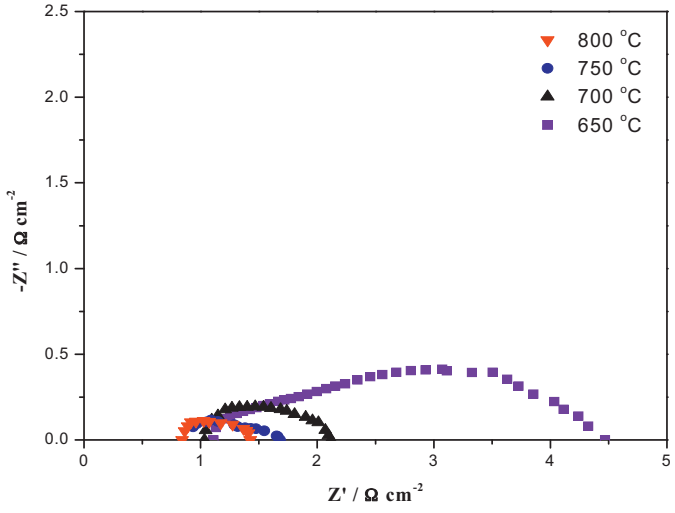

Fig. 5. Impedance spectra of HF-SOFC measured under open-circuit condition at 650–800 °C.

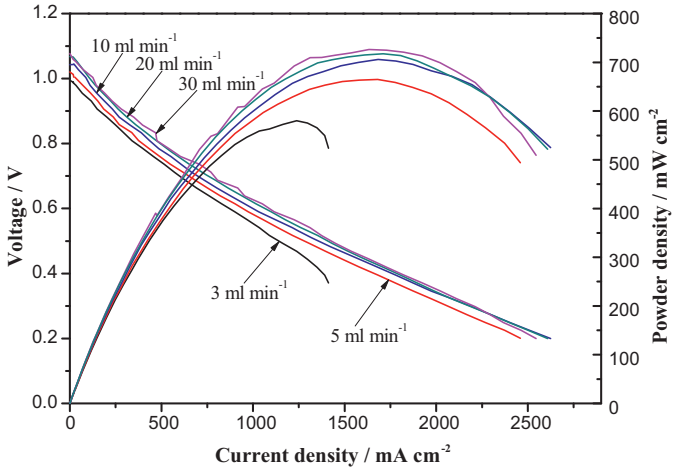

Fig. 7. Current–voltage characteristics and the corresponding power densities as a function of current densities for HF-SOFC at different fuel flow rate at 800 °C.

at the inner side of the hollow fiber provides fast channels to the electrolyte for the fuel gas and the sponge-like microporous structure near the YSZ electrolyte can provide large reduction catalysis area of H_2 and enlarge the area of the anode triple phase boundary including the anode, electrolyte and H_2 gas, which is a benefit for improving the total cell performance.

In order to further evaluate the performance of the as-prepared HF-SOFC, resistances of the cells were investigated by AC impedance spectroscopy under open-circuit conditions, as shown in Fig. 5. For the whole cell impedance, the high frequency intercept corresponds to the ohmic resistance (R_o) of the cell, while the low frequency intercept represents the total resistance of the cell (R_t) [29]. Therefore, between the high frequency and low frequency intercepts with the real axis is the interfacial polarization resistance (R_p) of the cell. The ohmic, polarization and total resistances acquired from the impedance spectra are summarized in Fig. 6. The ohmic resistance of YSZ electrolyte is 0.84, 0.92, 1.03 and 1.11 Ω cm^2 at 800, 750, 700 and 650 °C, respectively, so the O_2^- conductivity of YSZ electrolyte can be calculated by R_o and the thickness of electrolyte. The O_2^- conductivity of the electrolyte (YSZ) in this study is measured to be 7.7×10^{-4} S cm^{-1} at 800 °C.

YSZ electrolyte with thickness of ca. 6.5 μm is quite dense and thin, and is tightly connected to both anode and cathode. As expected, the ohmic resistances and polarization resistances significantly decrease with the increase of the operation temperature. For example the polarization resistance decreases from 3.36 Ω cm^2 to 0.58 Ω cm^2 when the temperature increases from 650 °C to at 800 °C.

Fig. 7 shows the performance of the HF-SOFC with different fuel flow rate at 800 °C using wet H_2. The maximum power densities are 580, 665, 706, 718 and 726 mW cm^{-2} at the fuel flow rate of 3, 5, 10, 20 and 30 mL min^{-1}, respectively. As the fuel flow increases, the maximum power density increases, especially in the low fuel flow range. The gas diffusion in the anode microstructure is apparently improved by the increase of fuel flow [30]. Additionally, the results are similar with those reported by Calise et al. [31]. In the range of high fuel flow rate, the increase of the maximum power density with the increase of fuel is not significant which is due to the gas diffusion limitation in the anode. According to the results, it was found that the fuel flow rate of 20 mL min^{-1} should be the optimal one for our cell.

Fig. 8 shows the fuel utilization at the maximum power output as a function of fuel flow rate at 800 °C. The fuel utilization was

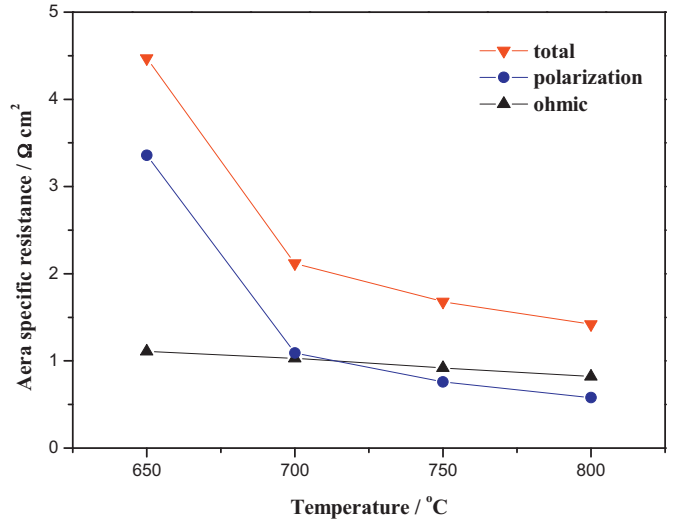

Fig. 6. Ohmic, polarization and total resistances determined from the impedance spectra of the HF-SOFC under open-circuit conditions at different temperatures.

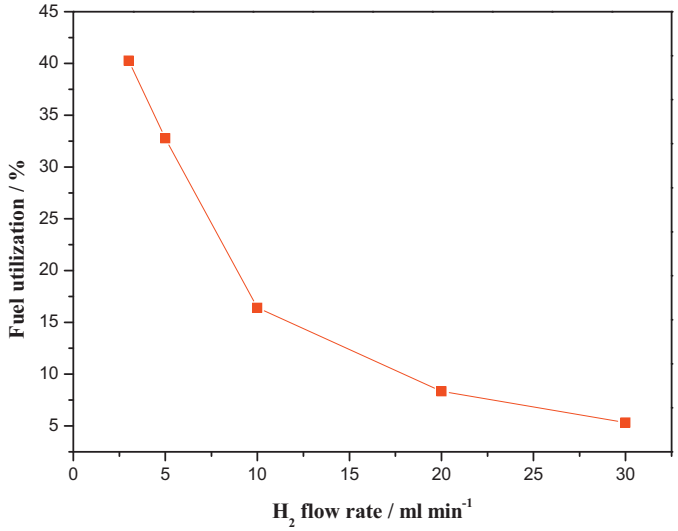

Fig. 8. Fuel utilization at the maximum power output as a function of fuel flow rate at 800 °C.

calculated from the fuel flow rates and the current at the maximum power density. We use the definition of fuel utilization (U_f) [32,33] as following:

$$U_f = \frac{I}{nFv} \quad (4)$$

where I, n, v and F are the current (A) drawn from the cell at peak power density, the number of electrons transferred in the reaction between hydrogen and oxygen ($n = 2$ for hydrogen), the flow rate of fuel (mol/s) and Faraday's constant, respectively. As can be seen, the fuel utilization efficiency of cell are calculated to be 40.26%, 32.76%, 16.41%, 8.34% and 5.31% at the fuel flow rate of 3, 5, 10, 20, and 30 mL min^{-1}, respectively. The low fuel utilization efficiency may be resulted from the non-recycling utilization of the fuel. On the other hand, the method used to calculate utilization (U_f) only considers the amount of fuel converted into externally useable electrical energy, the effective utilization calculated will therefore be slightly smaller than the amount of hydrogen reacted due to various losses incurred in the cell [34]. So, in order to maximize the output power of the cell, the fuel flow rate must be maintained high, however, it leads to low fuel utilization. The fuel utilization and the output power changed in the opposite direction as the fuel flow rate changed, thus, further optimization of the modules as well as system configuration is required [35]. In this case, the fuel should be recycled to improve the efficiency of fuel utilization.

4. Conclusion

An anode-supported asymmetric hollow fiber SOFC based on the YSZ electrolyte membrane and LSM–YSZ composite cathode has been prepared by the spinning/phase inversion and dip coating techniques with a co-sintering process. The asymmetric hollow fiber anode structure plays an important role in the electrochemical performance of HF-SOFC. When moist hydrogen (20 ml min^{-1}) as fuel and ambient air as oxidant were applied for the HF-SOFC, it generated maximum power densities of 285, 446, 549 and 708 mW cm^{-2} at 650, 700, 750 and 800 °C, respectively. The fuel utilization efficiency of cell are measured to be 40.26%, 32.76%, 16.41%, 8.34% and 5.31% at 800 °C at the fuel flow rate of 3, 5, 10, 20, and 30 mL min^{-1}, respectively. Such anode-supported HF-SOFCs are excellent candidates for smaller scale practical applications.

Acknowledgments

The authors greatly acknowledge the financial support by Natural Science Foundation of China (nos. U0834004, 20936001), the Science-Technology Plan of Guangzhou City (2009J1-C511-1) and the Fundamental Research Funds for the Central Universities, SCUT (no. 2009220038).

References

[1] O. Yamamoto, Electrochim. Acta 45 (2000) 2423–2435.
[2] Z.P. Shao, S.M. Haile, Nature 431 (2004) 170–173.
[3] Z.P. Shao, C.M. Zhang, W. Wang, C. Su, W. Zhou, Z.H. Zhu, H.J. Park, C. Kwak, Angew. Chem. Int. Ed. 50 (2011) 1792–1797.
[4] J. Ding, J. Liu, W.S. Yuan, Y.H. Zhang, J. Eur. Ceram. Soc. 28 (2008) 3113–3117.
[5] L. Zhang, H.Q. He, W.R. Kwek, J. Ma, E.H. Tang, S.P. Jiang, J. Am. Ceram. Soc. 92 (2009) 302–310.
[6] M.C. Williams, J.P. Strakey, S.C. Singhal, J. Power Sources 131 (2004) 79–85.
[7] N. Droushiotis, M. Othman, U. Doraswami, Z.T. Wu, G. Kelsall, K. Li, Electrochem. Commun. 11 (2009) 1799–1802.
[8] T. Yamaguchi, T. Suzuki, S. Shimizu, Y. Fujishiro, M. Awano, J. Membr. Sci. 300 (2007) 45–50.
[9] T. Suzuki, M.H. Zahir, T. Yamaguchi, Y. Fujishiro, M. Awano, N. Sammes, J. Power Sources 195 (2010) 7825–7828.
[10] S.B. Lee, T.H. Lim, R.H. Song, D.R. Shin, S.K. Dong, Int. J. Hydrogen Energy 33 (2008) 2330–2336.
[11] C.C. Wei, K. Li, Ind. Eng. Chem. Res. 47 (2008) 1506–1512.
[12] L. Zhao, X.Z. Zhang, B.B. He, B.B. Liu, C.R. Xia, J. Power Sources 196 (2011) 962–967.
[13] X.Z. Zhang, B. Lin, Y.H. Ling, Y.C. Dong, G.Y. Meng, X.Q. Liu, Int. J. Hydrogen Energy 35 (2010) 8654–8662.
[14] C.H. Yang, C. Jin, F.L. Chen, Electrochem. Commun. 12 (2010) 657–660.
[15] C.C. Wei, O.Y. Chen, Y. Liu, K. Li, J. Membr. Sci. 320 (2008) 191–197.
[16] T. Suzuki, T. Yamaguchi, Y. Fujishiro, M. Awano, J. Power Sources 160 (2006) 73–77.
[17] M.H.D. Othman, N. Droushiotis, Z.T. Wu, G. Kelsall, K. Li, Adv. Mater. 23 (2011) 2480–2483.
[18] N. Droushiotis, U. Doraswami, K. Kanawka, G.H. Kelsall, K. Li, Solid State Ionics 180 (2009) 1091–1099.
[19] M.H.D. Othman, N. Droushiotis, Z.T. Wu, G. Kelsall, K. Li, J. Power Sources 196 (2011) 5035–5044.
[20] C. Yang, W. Li, S. Zhang, L. Bi, R.R. Peng, C.S. Chen, W. Liu, J. Power Sources 187 (2009) 90–92.
[21] X.Z. Zhang, B. Lin, Y.H. Ling, Y.C. Dong, G.Y. Meng, X.Q. Liu, J. Alloys Compd. 497 (2010) 386–389.
[22] Y.Y. Wei, H.F. Liu, J. Xue, Z. Li, H.H. Wang, AIChE J. 57 (2011) 975–984.
[23] N.T. Yang, X.Y. Tan, Z.F. Ma, J. Power Sources 183 (2008) 14–19.
[24] J. Ding, J. Liu, J. Power Sources 193 (2009) 769–773.
[25] M. Khayet, Chem. Eng. Sci. 58 (2003) 3091–3104.
[26] U. Doraswami, P. Shearing, N. Droushiotis, K. Li, N.P. Brandon, G.H. Kelsall, Solid State Ionics 192 (2011) 494–500.
[27] V. Esposito, D.Z. de Florio, F.C. Fonseca, E.N.S. Muccillo, R. Muccillo, E. Traversa, J. Eur. Ceram. Soc. 25 (2005) 2637–2641.
[28] A. Kuzjukevics, S. Linderoth, Solid State Ionics 93 (1997) 255–261.
[29] T. Suzuki, Y. Funahashi, T. Yamaguchi, Y. Fujishiro, M. Awano, J. Power Sources 171 (2007) 92–95.
[30] T. Suzuki, Z. Hasan, Y. Funahashi, T. Yamaguchi, Y. Fujishiro, M. Awano, Science 325 (2009) 852–855.
[31] F. Calise, G. Restucccia, N. Sammes, J. Power Sources 195 (2010) 1163–1170.
[32] K.V. Galloway, N.M. Sammes, J. Electrochem. Soc. 156 (2009) B526–B531.
[33] S.C. Singhal, K. Kendall, High-Temperature Solid Oxide Fuel Cells: Fundamentals, Design and Applications, Elsevier Ltd., Oxford, 2003.
[34] K.S. Howe, G.J. Thompson, K. Kendall, J. Power Sources 196 (2011) 1677–1686.
[35] T. Suzuki, Y. Funahashi, T. Yamaguchi, Y. Fujishiro, M. Awanoa, J. Electrochem. Soc. 155 (2008) B1296–B1299.